HHS Public Access

Author manuscript

Ann Biomed Eng. Author manuscript; available in PMC 2016 August 01.

Published in final edited form as:

Ann Biomed Eng. 2015 August ; 43(8): 1918–1934. doi:10.1007/s10439-014-1212-4.

Six Degree of Freedom Measurements of Human Mild Traumatic Brain Injury

Fidel Hernandez[1], **Lyndia C. Wu**[2], **Michael C. Yip**[2], **Kaveh Laksari**[2], **Andrew R. Hoffman**[3], **Jaime Lopez**[4], **Gerald Grant**[5], **Svein Kleiven**[6], and **David B. Camarillo**[2]

[1]Department of Mechanical Engineering, Stanford University, Stanford, CA

[2]Department of Bioengineering, Stanford University, Stanford, CA

[3]Department of Medicine, Stanford University, Stanford, CA

[4]Department of Neurology, Stanford University, Stanford, CA

[5]Department of Neurosurgery, Stanford University, Stanford, CA

[6]Department of Neuronic Engineering, KTH Royal Institute of Technology, Stockholm, Sweden

Abstract

This preliminary study investigated whether direct measurement of head rotation improves prediction of mild traumatic brain injury (mTBI). Although many studies have implicated rotation as a primary cause of mTBI, regulatory safety standards use 3 degree of freedom (3DOF) translation-only kinematic criteria to predict injury. Direct 6DOF measurements of human head rotation (3DOF) and translation (3DOF) have not been previously available to examine whether additional DOFs improve injury prediction. We measured head impacts in American football, boxing, and mixed martial arts using 6DOF instrumented mouthguards, and predicted clinician-diagnosed injury using 12 existing kinematic criteria and 6 existing brain finite element (FE) criteria. Among 513 measured impacts were the first two 6DOF measurements of clinically-diagnosed mTBI. For this dataset, 6DOF criteria were most predictive of injury, more than 3DOF translation-only and 3DOF rotation-only criteria. Peak principal strain in the corpus callosum, a 6DOF FE criteria, was the strongest predictor, followed by two criteria that included rotation measurements, peak rotational acceleration magnitude and Head Impact Power (HIP). These results suggest head rotation measurements may improve injury prediction. However, more 6DOF data is needed to confirm this evaluation of existing injury criteria, and to develop new criteria that considers directional sensitivity to injury.

Keywords

concussion; mTBI; instrumented mouthguard; six degree of freedom measurements; kinematic criteria; finite element analysis; machine learning; translational acceleration; rotational acceleration; biomechanics

Correspondence: David Camarillo, Department of Bioengineering, Stanford University, 318 Campus Drive, Clark Center Room S170, Stanford, CA 94305-5444, Phone: 650-725-2590, Fax: 650-723-8544, dcamarillo@stanford.edu.

Conflict of Interest: None of the authors had any conflict of interest regarding this manuscript.

Introduction

According to the World Health Organization, more than 40 million people worldwide suffer a mild traumatic brain injury (mTBI) each year [15]. These injuries are classified as *focal* or *diffuse* to describe a wide spectrum of pathological outcomes and distinguish between distinct injury mechanisms. Focal injuries are common in unprotected falls and comprise lacerations, skull fracture, cerebral contusions and hemorrhage caused by concentrated contact forces [25,68]. In contrast, diffuse injuries may occur in the absence of concentrated contact forces, as in whiplash, blast exposure, or impact with a padded surface, and commonly describe cerebral concussion associated with inertial acceleration of the brain [18,48,60] As many as 3.8 million concussions occur in the United States each year during sports and recreation alone, and an estimated 50% of incidents may go unreported [34]. Neurodegenerative disease has been reported in soldiers, professional athletes, and more recently, amateur athletes who have experienced repeated injuries [17,28,31,36,73].

mTBI is thought to be caused by sudden translation and rotation of the head, but this motion has yet to be directly and independently measured in humans until now. In 1943, Holbourn first hypothesized that rapid rotation, and not translation, produces diffuse brain injury during blunt head trauma [37]. Assuming brain tissue and cerebrospinal fluid are incompressible inside the skull (like water or gel that fill a rigid vessel), Holbourn speculated that the brain does not deform due to pure head translation. He proposed the brain deforms considerably due to rotational acceleration because of its low shear modulus, a response that was recently demonstrated for normal head motion in a live human [6] and for concussive-severity head motion in a human cadaver [33]. While later studies confirmed that cerebral concussion and loss of consciousness (LOC) could be induced in primates with rotational acceleration, injuries were more severe when rotation was combined with translational contact trauma, possibly due to coupled pressure gradients and diffuse strain [62]. Moreover, animal and computational studies found tolerance to acceleration varies substantially by anatomical direction: coronal rotation produced more severe injuries in primates [26] and larger brainstem and corpus callosum tissue strains in a finite element (FE) model [46] while sagittal rotation produced more severe injuries in neonatal piglets (with different head and neck geometry) [11,20,74]. These studies suggest direct measurement of head rotation should capture directional components, and not just the magnitude, of rotational acceleration.

Although previous research has shed light on the potential mechanism of mTBI, there is a lack of consensus and supporting data for criteria to predict injury risk. Several (head) kinematic criteria and brain FE criteria have been previously proposed to predict the risk of mTBI (Table 1), but none have amassed widespread acceptance. Regulatory safety standards have traditionally used 3 degree of freedom (3D0F) translation-only kinematic criteria [21,45,51]. Criteria that use rotation measurements may better capture the mechanism of mTBI, but direct 6D0F measurements of human mTBI necessary to investigate this hypothesis have been previously unavailable (Table 2). Earlier efforts to measure or deduce human head kinematics in the field have employed headband-mounted sensors [50,64,67], helmet-mounted sensors [19,53,70], and laboratory reconstructions of impacts recorded in broadcast video [63]. However, these datasets are limited due to their indirect (dependent)

estimates of head rotation [8,19,50,53,67], measurement errors from non-rigid skull fixation [2,39,57], and restriction to test populations that typically wear helmets [7,69]. A few laboratory studies proposed the use of mouthpiece-mounted sensors as an alternative means of measuring head kinematics [5,35,52], but to the best of our knowledge, field data with these devices have not yet been published.

Our objective was to investigate whether direct measurement of head rotation improves prediction of mTBI. To that end, we measured 6DOF translational and rotational head kinematics using instrumented mouthguards that conformed and affixed to the upper dentition for a close approximation of skull motion. We used this preliminary data to evaluate the deviance of existing injury criteria from a perfectly-predictive model and investigate new approaches to injury prediction.

Materials and Methods

Athletes were fitted with instrumented mouthguards and monitored for symptoms of mild traumatic brain injury (mTBI) by trained clinicians. These devices monitored acceleration to determine if an impact occurred. When an impact triggered the device, six sensors recorded measurements to compare the data signatures of clinically-diagnosed injuries with other head impacts. Video-confirmed impact measurements were used to calculate kinematic criteria and estimate brain finite element (FE) criteria using finite element analysis. Injury prediction for each criteria was compared using univariate logistic regression. Finally, a novel multivariate machine learning approach to injury prediction was investigated.

Mouthguard design and impact detection

To detect impacts and investigate how impact forces combine to cause mTBI, we built instrumented mouthguards that measure six degree of freedom (6DOF) head kinematics (Fig. 1A). Each device contained a tri-axis accelerometer measuring translational acceleration in the anterior to posterior, left to right, and superior to inferior directions, and a tri-axis gyroscope measuring rotational velocity in the coronal, sagittal, and horizontal planes. Activity that exceeded a programmed accelerometer threshold was recorded and downloaded following each athletic event (game, practice, sparring session, or match). The threshold was chosen at 7 *g* (7 times gravity) or 10 *g* depending on the length of the athletic event, to maximize data collection with limited on-board memory (16 Mbit) and battery life. A microprocessor recorded time-stamped kinematic sensor measurements at 1 kHz for 10 ms prior to the triggering acceleration, and 90 ms post-trigger. The electronics were embedded in material that was fitted to each subject through a standard boil-and-bite process, or by pressure forming around the subject's dental mold. The custom fit provided a conforming, rigid coupling to the athlete's skull through the maxillary (upper) dentition, and estimates of head center of gravity kinematics. We used a laboratory head impact model and previously-published validation protocol to quantify the measurement accuracy of each mouthguard design used in the study [13].

Four mouthguard designs were used in the present study and validated against an anthropomorphic dummy head instrumented with a 6aω sensor package (Table 3) [13,41]. Design differences among the four models included form factor (sensors embedded in the

mouth, or sensors embedded in a cantilever tab between the lips), accelerometer (ADXL377, Analog Devices, Inc., Norwood, MA, USA, or H3LIS331DL, ST Microelectronics, Geneva, Switzerland), and gyroscope (L3G4200D, ST Microelectronics, Geneva, Switzerland, or ITG-3500A, InvenSense Inc., San Jose, CA, USA).

Video of all athletic events was used to purify the mouthguard dataset for investigation of injury biomechanics (Fig. 1B). Time-stamped high definition video (30 frames s^{-1}) captured the timing and sequence of head impacts. Using this video, activity recorded on the mouthguard was manually classified in two categories: head impacts and spurious triggers (Fig. 1C). Head impacts were defined as contact between a player's head and any foreign entity (another player's head, body, limb, or the ground). Only video-confirmed impacts were selected for analysis in the present study. Spurious triggers such as body contact, device insertion/removal, and device manual manipulation were rejected. High speed (1300-2500 frames s^{-1}) video was also recorded at select athletic events (Phantom Miro LC-320S, Vision Research, Wayne, NJ) to study head impacts with higher temporal resolution and for comparison to mouthguard measurements (Movies S1 and S2).

Mouthguard deployment and injury monitoring

We instrumented subjects who are exposed to repeated athletic head impacts over a wide spectrum of conditions. Of 31 recruited subjects, 28 were collegiate American football players, 2 were professional boxers (1 male and 1 female), and 1 was a male professional mixed martial artist. Prototype devices were deployed at 19 select athletic events over three years. Human subject protocols were approved by the Stanford Institutional Review Board (IRB No. 21304) and we received informed consent from all subjects.

At data collection events, subjects experiencing injury symptoms were monitored for potential brain injury. At competitions, sideline/ringside clinicians monitored subjects throughout the event. When signs of injury were identified by the clinician or self-reported by the subject, the clinician/trainer conducted an immediate neurological evaluation. If injury was suspected, the subject was removed from competition to receive a detailed neurological evaluation. At practices and training events, clinical or research staff were present to identify signs of brain injury throughout each event. In cases of injury, the subject was removed from the event and taken to a clinician for a detailed evaluation. Detailed evaluation following competition and training event injuries was conducted within 24 hours of injury and consisted of a 3 Tesla (3T) magnetic resonance imaging (MRI) scan and a neurological examination. During the neurological examination, the subject was asked to report the circumstances and symptoms relating to their injury. The neurological examination was repeated at 3 days and 3 months post-injury. In the absence of a clinically-diagnosed concussion, recorded head impacts were categorized as “non-injury”.

Mouthguard measurement processing

Raw accelerometer measurements of translational acceleration and raw gyroscope measurements of rotational velocity were filtered using a second-order Butterworth low-pass filter with a cutoff frequency of 200 Hz and 110 Hz, respectively [13]. Accelerometer measurements were defined as the acceleration of the accelerometer origin in accelerometer

reference frame. The gyroscope measurements were defined as the rotational velocity of gyroscope reference frame in ground inertial frame. Sensor origins were defined at the sensor location (Fig. 1) and their location relative to the center of gravity of the 50th percentile male (since MRI data was not available for all subjects) was determined using CAD drawings of the dummy head using for accuracy validation [13]. Sensor measurements were transformed to express the translational acceleration of the head center of gravity and the rotational velocity and acceleration of a head anatomical reference frame (pointing in the anterior, left, and superior directions) using a previously published algorithm [13].

Animations of the mouthguard measurements were generated in MATLAB (Mathworks, Natick, MA, USA) (Movies S1 and S2). The orientation and position of the head in the animation were generated by first estimating the head orientation in the first frame (t = 0 ms) of the video, and then integrating the accelerometer and gyroscope data from the mouthguards. This data was subsequently transformed to the center of gravity of the head to resolve the position and orientation of the head in future frames.

Kinematic injury criteria

Twelve existing kinematic injury criteria (Table 1) were calculated using the collected and processed 6DOF mouthguard measurement:

Peak Translational Acceleration Magnitude (a_{peak}) [18,30,50,60,63,71] was defined as the peak value of the translational acceleration vector magnitude time series,

$$a_{peak} = \max \|\vec{\boldsymbol{a}}(t)\| \quad (1)$$

where $\vec{\boldsymbol{a}}$ represents the translational acceleration vector (anterior, left, superior) and $\|\vec{\boldsymbol{a}}\|$ represents the magnitude (computed as L^2 norm) of a vector $\vec{\boldsymbol{a}}$. The maximum is taken over the entire 100 ms window when sensor measurements are recorded.

Head Injury Criterion (HIC_{15} and HIC_{36}) [21,45,51,63,78] is the most widely used injury criteria and was calculated as,

$$HIC = \max_{t_1,t_2} \left\{ \left[\frac{1}{t_2 - t_1} \int_{t_1}^{t_2} \|\vec{\boldsymbol{a}}(t)\| dt \right]^{2.5} (t_2 - t_1) \right\} \quad (2)$$

where $\|\vec{\boldsymbol{a}}(t)\|$ is the magnitude of translational acceleration and the times t_1 and t_2 are chosen to maximize the value of HIC, bounded by $t_2 - t_1 < 15$ ms for HIC_{15} or $t_2 - t_1 < 36$ ms for HIC_{36}.

Severity Index (SI) [7,8,23,51,63], also known as Gadd Severity Index (GSI), is given by,

$$SI = \int \|\vec{\boldsymbol{a}}(t)\|^{2.5} dt \quad (3)$$

The integral is evaluated over the period of time from when the signal first exceeds 4 g to when it returns to 4 g after the largest peak [51].

Peak Rotational Acceleration Magnitude (α_{peak}) [37,48,64,63,72] was defined as the peak value of the rotational acceleration vector magnitude time series,

$$\alpha_{peak} = \max \|\vec{\boldsymbol{\alpha}}(t)\| \quad (4)$$

Where $\vec{\boldsymbol{\alpha}}$ represents the rotational acceleration vector (coronal, sagittal, horizontal). The maximum is taken over the entire 100 ms window when sensor measurements are recorded.

Rotational Injury Criterion (RIC) [12,42] is the rotational acceleration equivalent of HIC and is defined as,

$$RIC = \max_{t_1,t_2} \left\{ \left[\frac{1}{t_2 - t_1} \int_{t_1}^{t_2} \|\vec{\boldsymbol{\alpha}}(t)\| dt \right]^{2.5} (t_2 - t_1) \right\} \quad (5)$$

where the times t_1 and t_2 are chosen to maximize the value of RIC, bounded by $t_2 - t_1 < 36$.

Peak Change in Rotational Velocity Magnitude ($\Delta\omega_{peak}$)[48,59,72] was defined as the largest change in rotational velocity magnitude,

$$\Delta\omega_{peak} = \|\vec{\boldsymbol{\omega}}(t)\| - \min \|\vec{\boldsymbol{\omega}}(t)\| \quad (6)$$

where $\vec{\boldsymbol{\omega}}$ represents the rotational velocity vector (coronal, sagittal, horizontal). The maximum and minimum is taken over the entire 100 ms window when sensor measurements are recorded.

Brain Injury Criterion (BrIC)[75] was developed by National Highway Traffic Safety Administration to account for diffuse axonal injury. It is based on Cumulative Strain Damage Measure (CSDM) values and uses critical values derived from finite element simulations:

$$BrIC = \frac{\vec{\boldsymbol{\omega}}_{peaks}}{\vec{\boldsymbol{\omega}}_{cr}} \quad (7)$$

where $\vec{\boldsymbol{\omega}}_{peaks}$ is a vector of the peak values for rotational velocity in each anatomical direction over time, and $\vec{\boldsymbol{\omega}}_{cr} = [\omega_{cr,x}, \omega_{cr,y}, \omega_{cr,z}] = [66.2, 59.1, 44.2]$ *rad/s* are the corresponding critical values determined from experimental data of frontal dummy impacts.

Head Impact Power (HIP) [49,55] is computed including translational and rotational components of acceleration at the head center of gravity, assuming rigid body motion, as shown below:

$$\begin{aligned} HIP = \max\, & (m\, a_x(t) \int a_x(t)dt + m\, a_y(t) \int a_y(t)dt \\ & + m\, a_z(t) \int a_z(t)dt + I_{xx}\, \alpha_x(t) \int \alpha_x(t)dt \\ & + I_{yy}\, \alpha_y(t) \int \alpha_y(t)dt + I_{zz}\, \alpha_z(t) \int a_z(t)dt) \end{aligned} \quad (8)$$

where *x, y, z* respectively correspond to anterior, left, superior for translation acceleration, and to coronal, sagittal, horizontal for rotational acceleration, $m = 4.5\ kg$ equals the mass of the human head, and $I_{xx}, I_{yy}, I_{zz} = [0.016, 0.024, 0.022]\ kg\ m^2$ equal the appropriate mass moments of inertia of the human head. The maximum is taken over the entire 100 ms window when sensor measurements are recorded.

Power Rotational Head Injury Criterion (PRHIC) [12,43] is similar HIC and RIC, and is defined as,

$$PRHIC = \max_{t_1,t_2} \left\{ \left[\frac{1}{t_2 - t_1} \int_{t_1}^{t_2} HIP_{rot}(t)\,dt \right]^{2.5} (t_2 - t_1) \right\} \quad (9)$$

where $HIP_{rot}(t)$ is the rotational acceleration contribution to Head Impact Power (HIP).

Generalized Acceleration Model for Brain Injury (GAMBIT) [54] is a generalized acceleration model for brain injury threshold that was previously proposed combining rotational and translational components of head acceleration and is calculated from the equation below,

$$GAMBIT = \max \left\{ \left[\left(\frac{\|\vec{\boldsymbol{\alpha}}(t)\|}{a_c} \right)^n + \left(\frac{\|\vec{\boldsymbol{\alpha}}(t)\|}{\alpha_c} \right)^m \right]^{1/s} \right\} \quad (10)$$

where a_c and α_c are the thresholds for the corresponding acceleration mode, and n, m and s are empirical values. The proposed values for above constants are $n = m = s = 2$, $a_c = 250\ g$, and $\alpha_c = 25000\ rad/s^2$ [54]. The maximum is taken over the entire 100 ms window when sensor measurements are recorded.

Principal Component Score (PCS) [29] is a weighted sum of translation and rotational accelerations, HIC, and SI with empirically determined weights, as shown below,

$$PCS = 10((0.4336\,\overline{a_{peak}} + 0.2164\,\overline{\alpha_{peak}}(13) + 0.4718\,\overline{SI} + 0.4742\,\overline{HIC}) + 2) \quad (11)$$

where X is a standardized value defined as $X = (X - \mu)/\sigma$, μ is the population mean, and σ is the population standard deviation.

Brain finite element (FE) criteria

To understand how head kinematics produce brain stress and strain, we simulated head impacts using a finite element (FE) head model developed at the KTH Royal Institute of Technology in Stockholm, Sweden [47], which represents an average adult male human head. This model, developed in LS-DYNA (LSTC, Livermore, CA), incorporates the scalp, skull, brain, meninges, cerebral spinal fluid, and eleven pairs of parasagittal bridging veins, differentiating between white matter, gray matter, and the ventricles. It models CNS tissues using an Ogden hyperelastic constitutive law (to account for large deformations of the tissue) with additional linear viscoelastic terms (to account for the rate dependence of the tissue). Also, the brain-skull interface is modeled by tied-node contact. The FE model was

validated against displacement data from cadaver head impact experiments performed by Hardy et al.[32], where neutral density targets were inserted inside cadaver brains and tracked using high-speed biplanar X-ray during impacts.

A subset of impacts were chosen for the computationally intense FE simulations (approximate 4 hour run-time for a single 100 ms impact on a high end workstation): all impacts resulting in clinically-diagnosed injury, a random sample of 10% of non-injury impacts, and all remaining impacts that exceeded any injury impact in at least one translational or rotational acceleration component. This subset of impacts is biased to include a greater percentage of non-injury impacts that would be most difficult to classify. For each simulation, 6DOF translational and rotational measurements over 100 ms were used as inputs to the model. Six existing brain deformation criteria (Table 1) were calculated using the results of the finite element simulations:

Peak Principal Strain (ε_{peak} and $\varepsilon_{peak,cc}$) [16,47] in the entire brain and in the corpus callosum was given by the first principal Green-Lagrange strain. This measure describes the maximum longitudinal tensile strain in the tissue and was calculated throughout the volume of the brain (and corpus callosum) over time. The peak was selected by taking the maximum over time across all individual model elements (in the whole brain and just in the corpus callosum) during a 100 ms interval.

Cumulative Strain Damage Measure ($CSDM_{15}$ and $CSDM_{25}$) [76] is a measure of the total volume fraction of brain tissue that undergoes strain values larger than a prescribed threshold (0.15 and 0.25 in our study).

Minimum/Maximum Pressure (P_{min} and P_{max}) [79] are the minimum and maximum values for pressure inside brain. In the present study, absolute value of each measure was used before performing statistical analysis.

Injury prediction using logistic regression

For each of the 18 kinematic and brain FE criteria, univariate logistic regression was performed to predict mTBI. For each impact, the criteria value was used as the predictor, and the clinical diagnosis of injury was used as a binary yes/no response. A generalized linear model regression (MATLAB's *glmfit* routine) of the responses, *y*, on the predictors, *x*, using a binomial distribution was performed in MATLAB for the following logistic model:

$$E(Y|x)=\frac{1}{(1+e^{-\beta_0-\beta_1 x})} \quad (12)$$

Where β_0 and β_1 are the intercept and slope coefficients, respectively. $E(Y|x)$ is the expected value of response Y given the predictor value x, or rather, the probability of injury for a given criteria value [38]. Logistic regression was performed on the subset of impacts for which finite element simulations were performed.

A Kolmogorov-Smirnov (KS) test of normality was performed on the natural log transform of each criteria, x'. For those criteria with log-normal distributions, the logistic model was also fit to standardized criteria values, $\hat{x}$, where,

$$\hat{x}=\frac{x'-\overline{x'}}{s'} \quad (13)$$

with $\overline{x'}$ and s' corresponding to the mean and standard deviation of the natural log transformed criteria values, x'. The corresponding intercept and slope coefficients, $\hat{\beta}_0$ and $\hat{\beta}_1$, describe the change in injury risk for a one standard deviation change in a given criteria.

The deviance (D) statistic assesses the quality of fit of a logistic regression (analogous to r^2 in linear regression) [38] and has been used to assess mTBI prediction (also known as -2LLR)[44,56,58,63]. The statistic is given by,

$$D=-2\ln\left(\frac{Likelihood\ of\ the\ fitted\ model}{Likelihood\ of\ the\ saturated\ model}\right) \quad (14)$$

where the predicted injury risk from a fitted model is that which is predicted by a given criteria, and predicted injury risk from a saturated model is equal to the observed injury risk (a perfectly-predictive model). For a binary prediction, the likelihood of the saturated model is equal to 1. As deviance approaches 0, the fitted model more closely approximates a perfectly-predictive model (the ratio of likelihoods inside the natural logarithm approaches 1). Zero deviance is expected for a criteria that perfectly classifies injury and non-injury impacts.

We computed the difference in deviance between each fitted model and a null model (predicted injury risk without using the criteria, that is, with only a β_0 term). This difference in deviance follows a χ^2 distribution; a low corresponding p-value suggested that a criteria significantly improved injury prediction [38]. A p-value is computed for the β_1 and $\hat{\beta}_1$ coefficients, with a low value indicating higher confidence that the β_1 parameter is not 0.

Injury prediction using machine learning

We investigated a novel approach to injury prediction using multivariate machine learning on kinematic measurements. Using the Support Vector Machine (SVM) classification routine defined in MATLAB's *svmtrain* and *svmclassify* functions, we determined an example multidimensional linear classifier separating the injury and non-injury impacts. Twelve input features were used in the routine: 3 direction components and magnitude of translational acceleration, rotational acceleration, and rotational velocity. Using the fewest features necessary, the routine finds a classification boundary (separating hyperplane) that maximizes the margins between the injury and non-injury classes.

Results

Injury diagnosis

Two subjects suffered a concussion during competitive play. The first patient was a 21-year-old male NCAA collegiate football player who sustained a concussion from a head impact while being tackled (Fig. 2A and Movie S1). The patient was witnessed to have brief extensor posturing of his upper extremities and loss of consciousness (LOC) lasting approximately 2 minutes. The patient continued to have an altered mental status with post concussive symptoms for 3 days post injury. His detailed neurological examination was normal. A 3T brain MRI was obtained within 24 hours and was normal. It was noted that this was his fourth overall concussion, and the second in 3 weeks. He did not return to play for the remaining two games of the season but ultimately made a complete recovery and now plays professionally. Follow up comprehensive neurological testing performed at 3 months post injury was normal.

The second patient was a 20-year-old male NCAA collegiate football player who sustained a concussion during practice. Although he did not lose consciousness, he self-reported several post concussive symptoms immediately following the impact including headache, poor concentration, and slowed reaction time. These symptoms persisted for 12 hours and then dissipated. Detailed neurological examination and 3T brain MRI at 18 hours post injury were normal. In retrospect, the patient reported suffering a mild head injury 48 hours prior to this impact, but he did not report his symptoms at the time. He ultimately made a full recovery and returned to football after a stepwise return to play.

Mouthguard measurements and kinematic criteria

Mouthguards were evaluated on a dummy head in the lab using a published validation protocol [13] (Table 3). Linear regression slopes (m) between mouthguard and dummy head peak magnitude measures were in the range 0.94 – 1.09 for all designs. The one-to-one linear model fit (quantified by r^2) was strongest for rotational velocity, followed by translational acceleration, then rotational acceleration. In field deployment, we collected data on volunteer subjects with each of the mouthguard designs. We measured a total of 513 video-confirmed head impacts: 421 from American football including two clinically-diagnosed injuries, 73 from boxing, and 19 from mixed martial arts (MMA). All three contact sports had similar distributions of kinematic measurements across all 513 impacts (Fig. S1). The 513 impacts were 1% of all mouthguard measurements recorded in the study, the rest being spurious triggers that were not included in the present analysis.

We collected 6DOF kinematic measurements of the clinically-diagnosed LOC injury (Fig. 2). The six acceleration time series were not simple impulses; the components reached local extrema, changed direction, and inflected many times in 100 ms, highlighting the complexity of forces acting on the subject's helmet, skull, and brain during the head impact. For the LOC injury, translational acceleration magnitude of the head (Fig. 2C) peaked at 106 g, rotational acceleration magnitude at 12900 rad s^{-2} (Fig. 2D), and change in rotational velocity magnitude at 34 rad s^{-1}. The self-reported injury was characterized by milder kinematics: 85 g, 7040 rad s^{-2}, and 23 rad s^{-1}.

These complex 6DOF measurements are traditionally reduced to 3DOF kinematic criteria such as peak translational acceleration (purple diamond) and HIC (gray shaded region) (Fig. 2C) to predict mTBI. We calculated these and ten other existing kinematic injury criteria (Table 1) for a subset of 110 head impacts: two injuries, 50 randomly-selected, and 58 with at least one translational or rotational acceleration component that exceeded either injury (Fig. 3); neither of the injured players had non-injury impacts in this group (accelerations exceeding their injury impacts). The log-normal median (μ) and interquartile range for peak translational acceleration magnitude was 33 *g* (21 - 53 *g*), for peak rotational acceleration magnitude was 2730 rad s^{-2} (1520 - 4880 rad s^{-2}), and for peak change in rotational velocity magnitude was 14 rad s^{-1} (9-22 rad s^{-1}), (Fig. 3A,E,G). The back-transformed (multiplicative) standard deviations (σ^*) for these statistics were 2.00, 2.37, and 1.90.

For the most widely-used injury criteria, HIC15 and HIC36, 3% and 4% of non-injury impacts exceeded the LOC injury, while 6% exceeded the self-reported injury (Fig. 3B and 3C, Eq. 2). Video analysis of these non-injury impacts revealed no remarkable incident. For peak rotational acceleration magnitude, 2% of the non-injury impacts exceeded the LOC injury, while 13% exceeded the self-reported injury. HIP (Fig. 3J, Eq. 8) considers both translation and rotation but had a similar distribution to peak rotational acceleration magnitude: 1% of non-injuries exceeded the LOC injury, while 9% exceeded the self-reported injury. More non-injury impacts exceeded the LOC in rotational acceleration than in HIP, however, the margin by which these impacts exceeded the LOC was greater in HIP than in rotational acceleration. The highest non-injury HIP (43 kW) was 48% above the LOC injury (29 kW), while the highest peak rotational acceleration (14300 rad s^{-1}) was 11% above the LOC (12900 rad s^{-1}).

Several non-injury impacts exceed the translational and rotational peak translational acceleration magnitude vectors (Figs. 3A, 4) of the LOC and self-reported injuries (7% and 13% of non-injury impacts, respectively). However, the injury accelerations occurred in unique directions (Fig. S2). The LOC injury was the largest peak translational acceleration vector (Fig. 4A - C) within a 70 degree cone, and the self-reported injury was largest within 20 degrees. The peak rotational acceleration vector of the LOC injury was even more unique, occurring largely in the coronal plane with no non-injuries of the same magnitude within a 150 degree cone (Fig. 4D-F). Direction components are weighted differently for only a few of the kinematic injury criteria evaluated here (Table 1), but are inherently factored into finite element analysis which models material and geometric asymmetries of the skull and brain.

Brain finite element (FE) criteria

For the same subset of 110 impacts, we estimated brain deformation using finite element (FE) simulations (Fig. 5, Movies S1 and S3). Peak principal strains for the LOC (49.8%) and self-reported (17.7%) injuries were higher than the non-injury median (16.4%, 10 - 27% interquartile range) over the entire brain (Fig. 5A). Maximum pressures for the LOC (83.7 kPa) and self-reported (40.0 kPa) injuries were also higher than the non-injury median (32.5 kPa, 20 -54 kPa interquartile range) (Fig. 5E). Minimum pressure (absolute value) for the

LOC (-91.2 kPa) and self-reported (-32.9 kPa) injuries exhibited the same trend compared to the non-injury median (24.5 kPa, -51 to -12 kPa interquartile range) (Fig. 5F).

The spatial distribution of strain for the LOC and self-reported injuries (Fig. 5G and 5H) indicated strain concentrations in the corpus callosum. Peak strains in non-injury impacts occurred more peripherally (Fig. 5K). The LOC (49.8%) and self-reported (17.7%,) injury strains in the corpus callosum were also higher the non-injury median (9.3%, 6 - 16% interquartile range). The LOC injury peak principal strain was among the highest in the subset of simulated impacts (top 6% for the whole brain and the highest in corpus callosum), while the self-reported injury was in the top 49% and 25% for the whole brain and corpus callosum, respectively. Although a few non-injury impacts produced strains in the corpus callosum that exceeded the self-reported injury (none exceeded the LOC injury), the injuries were the only impacts where the peak principal strain occurred in the corpus callosum (Fig. 5K). For both injuries, the largest pressure differential occurred between opposite sides of the brain, indicating the coup and contrecoup injury mechanism (Fig. 5I and 5J).

Injury prediction

Univariate logistic regression was used to predict injury for kinematic and FE criteria (Fig. 6), with a lower deviance statistic indicating a closer approximation to a perfectly-predictive model. The predictor with the lowest deviance was peak strain in the corpus callosum (13.5), a 6DOF FE criteria, followed by peak rotational acceleration magnitude (14.9), HIP (15.7), and GAMBIT (15.8), all criteria that include rotation measurements. These four criteria had deviance that were significantly ($\alpha = 0.05$) lower than the deviance of the null model (20.0). Among the translation-only criteria (red bars), peak acceleration had the lowest deviance (16.4); all groups that included rotation measures had at least one measure with lower deviance. For this limited injury dataset, rotational kinematics (whether alone or combined with translation) generally had lower deviance than translation-only criteria. Peak strain in the corpus callosum, peak rotational acceleration, and HIP also had the largest standardized regression coefficients, β_0 and β_1. That is, a standard deviation change in these criteria had the greatest effect on predicted injury risk (Fig. 6).

Multivariate machine learning and Support Vector Machine (SVM) classification provided an alternative approach to injury prediction. Of the 12 kinematic features used to train the SVM classifier, a minimum of three were required to produce a dichotomous hyperplane boundary between injury and non-injury (Fig. 7). Two of these kinematic features, inferior-superior and anterior-posterior translational acceleration, defined a plane in which the LOC and self-reported injuries were nearly unique. A few non-injury impacts were higher magnitude in this plane, but the addition of coronal rotational acceleration was sufficient to unambiguously classify the injuries. With only two injuries to train the classifier, this plane should in no way be viewed as describing an injury threshold boundary. Rather, this plane illustrates a different approach to binary injury prediction allowing for optimally solved directional weightings of acceleration components.

Discussion

The objective of this study was to investigate whether direct measurement of head rotation improves mTBI prediction. Using an instrumented mouthguard, we reported the first direct six degree of freedom (6DOF) measurements of clinically-diagnosed mTBI and assessed predictive deviance of several existing injury criteria using univariate logistic regression. Criteria that included rotation gave the lowest deviance, principal strain in the corpus callosum (6DOF), α_{peak} (3DOF), HIP (6DOF), and GAMBIT (6DOF), better than any translation-only criteria. While prior studies have included 2DOF head rotation estimates (inferior-superior axis excluded) [8,19,72], these are not directly measured, but rather, determined empirically as a function of translational measurements by assuming rotation about a fixed point in the neck [72]. In the current study, only four criteria significantly improved prediction over a null model without any criteria, and they all use full 3DOF rotation measurements. Brain strain has been attributed to head rotation [40,46], which is consistent with our observation that principal strain in the corpus callosum had the greatest predictive accuracy, followed by peak rotational acceleration. Brain pressure has been attributed to head translation [40,46,80] and we observed maximum and minimum pressure to have some of the lowest predictive accuracies. FE criteria, rotational acceleration, and HIP have in common that they all have a physical basis in torque, power, and deformation. Given the small injury sample size, we did not attempt to determine absolute injury risk, or suggest any injury thresholds. That is, we did not use our regression parameters to propose criteria values associated with any specific likelihood of injury.

The criteria with the highest deviance were PRHIC, BrIC and the whole brain finite element (FE) values. PRHIC is a rotational kinematic criterion adapted from HIC that also assumes a power exponent of 2.5. However unlike the HIC exponent, the PRHIC exponent was not empirically determined since 6DOF injury data was not available at the time PRHIC was proposed [43], potentially explaining the higher deviance. BrIC was developed based on correlation with the FE outputs CSDM and peak strain. We found that CSDM and peak strain outputs of the KTH FE model had a similarly low predictive accuracy as BrIC. CSDM was originally developed using the SIMon FE model, but it was proposed as a model-independent measure of whole brain deformation [75,76] and has been previously estimated using the KTH FE model[47] Although the KTH and SIMon models have been validated against the same datasets, their prediction of brain deformation may differ [40]. The KTH FE model was used for all simulations in the present study and is expected to provide consistent relative responses across subjects.

Strain in the corpus callosum resulted in lower deviance than whole brain FE criteria but was still an imperfect injury predictor. However, the two injuries were the only impacts analyzed whose peak strain occurred in the corpus callosum. The injuries had large coronal rotation components that may have produced a wave down the falx that gave rise to stress where it meets the corpus callosum. These findings are consistent with the critical function of the corpus callosum to transmit information between cerebral hemispheres. Callosal damage disrupts this communication, affecting perception [24] and causing traditional symptoms of mTBI such as disorientation, amnesia, and impaired visual judgment [77]. Recently, diffusion tensor imaging found that disruption in the corpus callosum impaired

performance after brain trauma, both in cognitive tasks and reaction time [4]. The axonal fibers in the corpus callosum responsible for this interhemispheric communication are highly organized directionally left-right. Fiber orientation results in material property anisotropy [3,22] but this was not modeled here, nor was the direction of the strain considered which certainly would have altered our results [27]. FE is a promising tool for predicting injury but may need to be specific in terms of tissue orientations and anatomical structures that cause the symptoms of injury. A validated FE model that utilizes the 6DOF data is important to derive tissue-level responses that kinematics data alone could not provide otherwise.

Although 3DOF translation-only criteria had higher deviance than those that included rotation, rotational criteria predictions could still be improved. It is important to note that these criteria were developed in the absence of human 6DOF direct measurements of injury. New criteria may be possible with the availability of more 6DOF data that could improve injury prediction. In addition to evaluating the effect of rotation, 6DOF data allows for the traumatic effects of rotation and translation in different directions to be evaluated. Animal research has shown that injury susceptibility can vary substantially depending on rotational direction [20,26,45,74]. Among the criteria we evaluated in this study, only PRHIC, BrIC, HIP, and the FE values differentiate among directions. These criteria, and their directional sensitivities, are physically based; PRHIC and HIP compute rotational power which varies in directions based on moment of inertia, while BrIC and FE vary in direction based on geometrical and material property asymmetries. It is indeed possible that refinement of the physics of these criteria will improve prediction when provided 6DOF measurements as input. However, the relationship between physical forces and cognitive symptoms is complex and can also be investigated from a data mining approach that learns directional sensitivity based on training data [29].

We explored a new machine learning approach to injury prediction by training an SVM binary classifier on kinematic measurements. SVM classification has been used previously to detect injury through video [66], CT image features [65], MRI image features [10], and electroencephalography features [14]. The machine learning classification algorithm presented here optimizes a combination of 12 kinematic measurements to best predict clinically-diagnosed injury, agnostic of the underlying physics. This approach is clinically-relevant as field decisions to triage the injured is a yes-no binary decision. The two injuries could be divided from the noninjury with a plane with three linearly weighted kinematic measurements. Given the small sample size of this study, this plane certainly does not suggest an injury tolerance. To define injury tolerance, SVM requires a larger sample of impacts that lie on the “boundary” between injury and non-injury (that is, SVM may not select certain injury impacts to define a classifier if they are obviously removed from the non-injury group, and vice versa). More injury data points will almost certainly require a higher dimensional hyperplane and possibly non-linear surface. Furthermore, temporal measures may be important as well since the brain is a dynamic system which may be more sensitive to pulses of certain durations. However, a statistical approach like this that factors in 6DOF spatiotemporal data independently may allow for new predictors to be developed that can more clearly distinguish injury. More 6DOF data will be required for such machine learning approaches to have more predictive value than (or with) physical approaches.

This study has several limitations to mention. The greatest limitation is small sample size of injury data making our findings only preliminary. For the injuries that were recorded, recent history of injury for both subjects could have reduced their tolerance to the injury that was measured [1,9,31]. Unfortunately, this type of patient history is very common in football. Similarly, concussive symptoms may have been experienced but not reported for other subjects on impacts labeled as non-injury. Furthermore, the instrumented mouthguard used in this study has been evaluated for accuracy in a laboratory setting with an anthropomorphic test device that has a fixed jaw [13]. While the design of the mouthguard is intended to fit tightly to the upper dentition, it is possible that mouthguard dislocation could occur leading to over- or under-estimation of acceleration signals that is beyond the bounds of the laboratory study. It is not possible to know with total certainty whether the injuries (or non-injury impacts) are direct measurement of skull accelerations, however, the signals were consistent with other experimental data from dummy head-mounted reference sensors. While the FE model used has been validated on cadaver data, it may not represent general in vivo properties or subject specific anatomy of those evaluated in this study. Only a subset of the recorded impacts were simulated in FE, including those with the highest level of acceleration. Finally, there was selection bias for the non-injury dataset given the time-intensive nature of video analysis; this dataset is enriched for injuries and therefore a subset of non-injury impacts was used in logistic regression to suggest injury probabilities.

Despite these limitations, this preliminary study of direct 6DOF measurements of mTBI suggests that rotational measurement does improve injury prediction using existing injury criteria. However, the predictive deviance of rotational measures was imperfect and may be improved by building/refining physical and/or statistical injury criteria. The importance of head translation and rotation in specific directions will not have consensus until more data is collected and tested on existing and new criteria.

Supplementary Material

Refer to Web version on PubMed Central for supplementary material.

Acknowledgments

We thank the Stanford Department of Athletics (Palo Alto, CA) for enabling this research, notably Scott Anderson, Director of Athletic Training, and Mike Gleeson, Video Director. We thank Kevin Bui and Bradley Hammoor for work in processing the event video, Joseph Schooler for coordinating human subject protocols, and Maria Malone for device manufacturing and deployment. We thank X2 Biosystems (Seattle, WA) for early device prototypes and continual support. We thank Roy Englebrecht Promotions (Newport Beach, CA) and B Street Boxing (San Mateo, CA) for help with subject recruitment. The study was supported by the National Institutes of Health (NIH) National Institute of Biomedical Imaging and Bioengineering (NIBIB) 3R21EB01761101S1, David and Lucile Packard Foundation 38454, Child Health Research Institute of Stanford University, and NIH ULI TR000093 for biostatistics consultation.

References

1. Abrahams S, Mc Fie S, Patricios J, Posthumus M, September AV. Risk factors for sports concussion: an evidence-based systematic review. Br J Sports Med. 2013
2. Allison MA, Kang YS, Bolte JH, Maltese MR, Arbogast KB. Validation of a helmet-based system to measure head impact biomechanics in ice hockey. Med Sci Sports Exerc. 2014; 46(1):115–23. [PubMed: 23846161]

3. Arbogast KB, Margulies SS. Material characterization of the brainstem from oscillatory shear tests. J Biomech. 1998; 31(9):801–7. [PubMed: 9802780]
4. Arenth PM, Russell KC, Scanlon JM, Kessler LJ, Ricker JH. Corpus callosum integrity and neuropsychological performance after traumatic brain injury: a diffusion tensor imaging study. J Head Trauma Rehabil. 2013; 29(2)
5. Bartsch A, Samorezov S. Cleveland Clinic “Intelligent Mouthguard”: A new technology to accurately measure head impact in athletes and soldiers. Proc SPIE 8723, Sensing Technologies for Global Health, Military Medicine, and Environmental Monitoring III, 87230N. 2013
6. Bayly PV, Cohen T, Leister E, Ajo D, Leuthhardt E, Genin G. Deformation of the human brain induced by mild acceleration. J Neurotrauma. 2005; 22(8):845–856. [PubMed: 16083352]
7. Beckwith JG, Chu JJ, Greenwald RM. Validation of a noninvasive system for measuring head acceleration for use during boxing competition. J Appl Biomech. 2007; 23(3):238–44. [PubMed: 18089922]
8. Beckwith JG, Greenwald RM, Chu JJ. Measuring head kinematics in football: correlation between the head impact telemetry system and Hybrid III headform. Ann Biomed Eng. 2012; 40(1):237–48. [PubMed: 21994068]
9. Beckwith JG, Greenwald RM, Chu JJ, Crisco JJ, Rowson S, Duma SM, Broglio SP, Mcallister TW, Guskiewicz KM, Mihalik JP, Anderson S, Schnebel B, Brolinson PG. Timing of concussion diagnosis is related to head impact exposure prior to injury. Med Sci Sports Exerc. 2013; 45(4): 747–754. [PubMed: 23135364]
10. Bianchi A, Bhanu B, Obenaus A. Dynamic low-level context for the detection of mild traumatic brain injury. IEEE Trans Biomed Eng. 2014:9294(c).
11. Browne KD, Chen X, Meaney DF, Smith DH. Mild traumatic brain injury and diffuse axonal injury in swine. J Neurotrauma. 2011; 28(9):1747–55. [PubMed: 21740133]
12. Caccese V, Ferguson J, Lloyd J, Edgecomb M, Seidi M, Hajiaghamemar M. Response of an impact test apparatus for fall protective headgear testing using a Hybrid-Ill head/neck assembly. Exp Techniques. 2014
13. Camarillo DB, Shull PB, Mattson J, Shultz R, Garza D. An instrumented mouthguard for measuring linear and angular head impact kinematics in American football. Ann Biomed Eng. 2013; 41(9):1939–49. [PubMed: 23604848]
14. Cao C, Tutwiler RL, Slobounov S. Automatic classification of athletes with residual functional deficits following concussion by means of EEG signal using support vector machine. IEEE Trans Neural Syst Rehabil Eng. 2008; 16(4):327–35. [PubMed: 18701381]
15. Cassidy JD, Carroll LJ, Peloso PM, Borg J, von Holst H, Holm L, Kraus J, Coronado V. Incidence, risk factors and prevention of mild traumatic brain injury: results of the WHO Collaborating Centre Task Force on Mild Traumatic Brain Injury. J Rehabil Med. 2004; (43 Suppl):28–60. [PubMed: 15083870]
16. Coats B, Eucker SA, Sullivan S, Margulies SS. Finite element model predictions of intracranial hemorrhage from non-impact, rapid head rotations in the piglet. Int J Dev Neurosci. 2012; 30(3): 191–200. [PubMed: 22239917]
17. DeKosky ST, Blennow K, Ikonomovic MD, Gandy S. Acute and chronic traumatic encephalopathies: pathogenesis and biomarkers. Nat Rev Neurol. 2013; 9(4):192–200. [PubMed: 23558985]
18. Denny-Brown DE, Russell WR. Experimental cerebral concussion. Brain. 1941; 64(2-3):93–164.
19. Duma SM, Manoogian SJ, Bussone WR, Brolinson PG, Goforth MW, Donnenwerth JJ, Greenwald RM, Chu JJ, Crisco JJ. Analysis of real-time head accelerations in collegiate football players. Clin J Sports Med. 2005; 15(1):3–8.
20. Eucker SA, Smith C, Ralston J, Friess SH, Margulies SS. Physiological and histopathological responses following closed rotational head injury depend on direction of head motion. Exp Neurol. 2011; 227(1):79–88. [PubMed: 20875409]
21. Federal Motor Vehicle Safety Standards (FMVSS). 571.202a. Section 571, Standard 202a - Head restraints. 2014

22. Feng Y, Okamoto RJ, Namani R, Genin GM, Bayly PV. Measurements of mechanical anisotropy in brain tissue and implications for transversely isotropic material models of white matter. J Mech Behav Biomed Mater. 2013; 23:117–32. [PubMed: 23680651]
23. Gadd C. Use of a weighted impulse criterion for estimating injury hazard. Proc of the 10th Stapp Car Crash Conference. 1966:164–174.
24. Gazzaniga, M.; Irvy, RB.; Mangun, GR. Cognitive Neuroscience The Biology of the Mind. W. W. Norton & Company; New York, NY: 1998.
25. Gennarelli TA. Mechanisms of brain injury. J Emerg Med. 1992; 11:5–11. [PubMed: 8445204]
26. Gennarelli TA, Thibault LE, Adams JH, Graham DI, Thompson CJ, Marcincin RP. Diffuse axonal injury and traumatic coma in the primate. Ann Neurol. 1982; 12(6):564–74. [PubMed: 7159060]
27. Giordano C, Kleiven S. Connecting fractional anisotropy from medical images with mechanical anisotropy of a hyperviscoelastic fibre-reinforced constitutive model for brain tissue. J R Soc Interface. 2013; 11(20130914)
28. Goldstein LE, Fisher AM, Tagge CA, Zhang XL, Velisek L, Sullivan JA, Upreti C, Kracht JM, Ericsson M, Wojnarowicz MW, Goletiani CJ, Maglakelidze GM, Casey N, Moncaster JA, Minaeva O, Moir RD, Nowinski CJ, Stern RA, Cantu RC, Geiling J, Blusztajn JK, Wolozin BL, Ikezu T, Stein TD, Budson AE, Kowall NW, Chargin D, Sharon A, Saman S, Hall GF, Moss WC, Cleveland RO, Tanzi RE, Stanton PK, McKee AC. Chronic traumatic encephalopathy in blast-exposed military veterans and a blast neurotrauma mouse model. Sci Transl Med. 2012; 4(134): 134–60.
29. Greenwald R, Gwin J, Chu J, Crisco J. Head impact severity measures for evaluating mild traumatic brain injury risk exposure. Neurosurgery. 2008; 62(4):789–798. [PubMed: 18496184]
30. Gurdjian ES, Lissner HR, Latimer FR, Haddad BF, Webster JE. Quantitative determination of acceleration and intracranial pressure in experimental head injury; preliminary report. Neurology. 1953; 3(6):417–23. [PubMed: 13054875]
31. Guskiewicz KM, McCrea M, Marshall SW, Cantu RC, Randolph C, Barr W, Onate JA, Kelly JP. Cumulative effects associated with recurrent concussion in collegiate football players: the NCAA Concussion Study. JAMA. 2003; 290(19):2549–2555. [PubMed: 14625331]
32. Hardy WN, Foster CD, Mason MJ, Yang KH, King AI, Tashman S. Investigation of head injury mechanisms using neutral density technology and high-speed biplanar x-ray. Stopp Car Crash J. 2001; 45:337–68.
33. Hardy WN, Mason MJ, Foster CD, Shah CS, Kopacz JM, Yang H, King AI, Bishop J, Bey M. A study of the response of the human cadaver head to impact. Stopp Car Crash J. 2008; 51:17–80.
34. Harmon KG, Drezner Ja, Gammons M, Guskiewicz KM, Halstead M, Herring Sa, Kutcher JS, Pana A, Putukian M, Roberts WO. American Medical Society for Sports Medicine position statement: concussion in sport. Br J Sports Med. 2013; 47(1):15–26. [PubMed: 23243113]
35. Higgins M, Halstead PD, Snyder-Mackler L, Barlow D. Measurement of impact acceleration: mouthpiece accelerometer versus helmet accelerometer. J Athl Train. 2007; 42(1):5–10. [PubMed: 17597937]
36. Hoge CW, McGurk D, Thomas JL, Cox AL, Engel CC, Castro CA. Mild traumatic brain injury in U.S. Soldiers returning from Iraq. N Engl J Med. 2008; 358(5):453–463. [PubMed: 18234750]
37. Holbourn AHS. Mechanics of head injuries. Lancet. 1943; 242(6267):438–441.
38. Hosmer, DW.; Lemeshow, S.; Sturdivant, RX. Applied Logistic Regression. 3rd. John Wiley & Sons, Inc.; Hoboken, NJ: 2013.
39. Jadischke R, Viano DC, Dau N, King AI, McCarthy J. On the accuracy of the Head Impact Telemetry (HIT) System used in football helmets. J Biomech. 2013; 46(13):2310–5. [PubMed: 23891566]
40. Ji S, Ghadyani H, Bolander RP, Beckwith JG, Ford JC, McAllister TW, Flashman LA, Paulsen KD, Ernstrom K, Jain S, Raman R, Zhang L, Greenwald RM. Parametric comparisons of intracranial mechanical responses from three validated finite element models of the human head. Ann Biomed Eng. 2014; 42(1):11–24. [PubMed: 24077860]
41. Kang Y, Moorhouse K, Bolte JH. Measurement of six degrees of freedom head kinematics in impact conditions employing six accelerometers and three angular rate sensors (6aω configuration). J Biomech Eng. 2011; 133(11):111007. [PubMed: 22168739]

42. Kimpara H, Iwamoto M. Mild traumatic brain injury predictors based on angular accelerations during impacts. Ann Biomed Eng. 2012; 40(1):114–26. [PubMed: 21994065]
43. Kimpara H, Nakahira Y, Iwamoto M. Head injury prediction methods based on 6 degree of freedom head acceleration measurements during impact. 2011; 2:13–19.
44. King AI, Yang KH, Zhang L, Hardy W, Viano DC. Is head injury caused by linear or angular acceleration? Proceedings of the 2003 International IRCOBI Conference on the Biomechanics of Impact". 2003 Sep.:1–12.
45. Kleinberger, M.; Sun, E.; Eppinger, R.; Kuppa, S.; Saul, R. Development of Improved Injury Criteria for the Assessment of Advanced Automotive Restraint Systems. National Highway Traffic Safety Administration; Washington, D.C.: 1998. Head Injury Criteria; p. 12-17.
46. Kleiven S. Evaluation of head injury criteria using a finite element model validated against experiments on localized brain motion, intracerebral acceleration, and intracranial pressure. Int J Crashworthines. 2006; 11(1):65–79.
47. Kleiven S. Predictors for traumatic brain injuries evaluated through accident reconstructions. Stopp Car Crash J. 2007; 51:81–114.
48. Margulies SS, Thubault LE. A proposed tolerance criterion for diffuse axonal injury in man. J Biomech. 1992; 25(8):917–23. [PubMed: 1639835]
49. Marjoux D, Baumgartner D, Deck C, Willinger R. Head injury prediction capability of the HIC, HIP, SIMon and ULP criteria. AccidAnal Prev. 2008; 40(3):1135–48.
50. Moon DW, Beedle CW, Kovacic CR. Peak head acceleration of athletes during competition - football. Med Sci Sports. 1971; 3(1):44–50. [PubMed: 5095335]
51. National Operating Committee on Standards for Athletic Equipment (NOCSAE). Standard Test Method and Equipment Used in Evaluating the Performance Characteristics of Protective Headgear/Equipment. 2012 Paper No. ND001-11m12.
52. Naunheim RS, Bayly PV, Standeven J, Neubauer JS, Lewis LM, Genin GM. Linear and angular head accelerations during heading of a soccer ball. Med Sci Sports Exerc. 2003; 35(8):1406–12. [PubMed: 12900697]
53. Naunheim RS, Standeven J, Richter C, Lewis LM. Comparison of impact data in hockey, football, and soccer. J Trauma. 2000; 48(5):938–41. [PubMed: 10823540]
54. Newman J. A generalized acceleration model for brain injury threshold (GAMBIT). Proceedings of the 1986 International IRCOBI Conference on the Biomechanics of Impact. 1986:121–131.
55. Newman J, Shewchenko N, Welbourne E. A proposed new biomechanical head injury assessment function-the maximum power index. Stapp Car Crash J. 2000a; 44:215–247. [PubMed: 17458729]
56. Newman JA, Barr C, Beusenberg M, Fournier E, Shewchenko N, Welbourne E, Withnall C. A new biomechanical assessment of mild traumatic brain injury. Part 2: Results and conclusions. Proceedings of the 2000 International IRCOBI Conference on the Biomechanics of Impact. 2000b: 223–233.
57. Newman JA, Beusenberg MC, Shewchenko N, Withnall C, Fournier E. Verification of biomechanical methods employed in a comprehensive study of mild traumatic brain injury and the effectiveness of American football helmets. J Biomech. 2005; 38(7):1469–81. [PubMed: 15922758]
58. Newman JA, Shewchenko N, Welbourne E. A proposed new biomechanical head injury assessment function - The Maximum Power Index. Stapp Car Crash J. 2000c; 44(724):362.
59. Ommaya A, Hirsch A. Tolerances for cerebral concussion from head impact and whiplash in primates. J Biomech. 1971; 4(1):13–21. [PubMed: 5001829]
60. Ommaya A, Hirsch A, Flamm E, Mahone R. Cerebral concussion in the monkey: an experimental model. Science. 1966; 153(3732):211–2. [PubMed: 4957321]
61. Ommaya AK, Faas F, Yarnell P. Whiplash injury and brain damage: an experimental study. JAMA. 1968; 204(4):285–289. [PubMed: 4967499]
62. Ommaya AK, Gennarelli TA. Cerebral concussion and traumatic unconsciousness. Correlation of experimental and clinical observations of blunt head injuries. Brain. 1974; 97(4):633–654. [PubMed: 4215541]

63. Pellman EJ, Viano DC, Tucker AM, Casson IR. Concussion in professional football, Part 1: Reconstruction of game impacts and injuries. Neurosurgery. 2003; 53(4):799–812. [PubMed: 14519212]
64. Pincemaille Y, Trosseille X, Mack P, Tarriere C, Breton F, Renault B, Recherche, U. R. A. U. D., and Pathologie, C. Some new data related to human tolerance obtained from volunteer boxers. Proc of the 33rd Stopp Car Crash Conference, SAE Paper No. 892435. 1989:177–190.
65. Prichep L, Jacquin A. Classification of traumatic brain injury severity using informed data reduction in a series of binary classifier algorithms. IEEE Trans Neural Syst Rehabil Eng. 2012 Nov.:806–822. [PubMed: 22855231]
66. Qian H, Mao Y, Xiang W, Wang Z. Home environment fall detection system based on a cascaded multi-SVM classifier. Proc of the 10th IEEE Conference on Control, Automation, Robotics and Vision. 2008 Dec.:17–20.
67. Reid SE, Epstein HM, O'Dea TJ, Louis MW. Head protection in football. J Sports Med. 1974; 2(2):86–92. [PubMed: 1186180]
68. Roth TL, Nayak D, Atanasijevic T, Koretsky AP, Latour LL, McGavern DB. Transcranial amelioration of inflammation and cell death after brain injury. Nature. 2014; 505(7482):223–8. [PubMed: 24317693]
69. Rowson S, Beckwith JG, Chu JJ, Leonard DS, Greenwald RM, Duma SM. A six degree of freedom head acceleration measurement device for use in football. J Appl Biomech. 2011; 27(1): 8–14. [PubMed: 21451177]
70. Rowson S, Brolinson G, Goforth M, Dietter D, Duma SM. Linear and angular head acceleration measurements in collegiate football. J Biomech Eng. 2009; 131(6):061016. [PubMed: 19449970]
71. Rowson S, Duma SM. Development of the STAR evaluation system for football helmets: integrating player head impact exposure and risk of concussion. Ann Biomed Eng. 2011; 39(8): 2130–40. [PubMed: 21553135]
72. Rowson S, Duma SM, Beckwith JG, Chu JJ, Greenwald RM, Crisco JJ, Brolinson PG, Duhaime AC, McAllister TW, Maerlender AC. Rotational head kinematics in football impacts: an injury risk function for concussion. Ann Biomed Eng. 2012; 40(1):1–13. [PubMed: 22012081]
73. Smith DH, Johnson VE, Stewart W. Chronic neuropathologies of single and repetitive TBI: substrates of dementia? Nat Rev Neurol. 2013; 9(4):211–21. [PubMed: 23458973]
74. Smith DH, Nonaka M, Miller R, Leoni M, Chen XH, Alsop D, Meaney DF. Immediate coma following inertial brain injury dependent on axonal damage in the brainstem. J Neurosurg. 2000; 93(2):315–22. [PubMed: 10930019]
75. Takhounts EG, Craig MJ, Moorhouse K, Mcfadden J, Hasija V. Development of Brain Injury Criteria (BrIC). 2013 Nov.57:1–24.
76. Takhounts EG, Ridella Sa, Hasija V, Tannous RE, Campbell JQ, Malone D, Danelson K, Stitzel J, Rowson S, Duma S. Investigation of traumatic brain injuries using the next generation of simulated injury monitor (SIMon) finite element head model. Stopp Car Crash J. 2008 Nov.52:1–31.
77. Ungerleider, LG.; Mishkin, M. Analysis of Visual Behavior. MIT Press; Cambridge, MA: 1982. Two cortical visual systems; p. 549-86.
78. Versace J. A review of the Severity Index. Proc of the 15th Stopp Car Crash Conference, SAE Paper No. 710881. 1971:771–796.
79. Ward C, Chan M, Nahum A. Intracranial pressure–a brain injury criterion. Stopp Car Crash J. 1980
80. Zhang L, Yang KH, King AI. A proposed injury threshold for mild traumatic brain injury. J Biomech Eng. 2004; 126(2):226. [PubMed: 15179853]

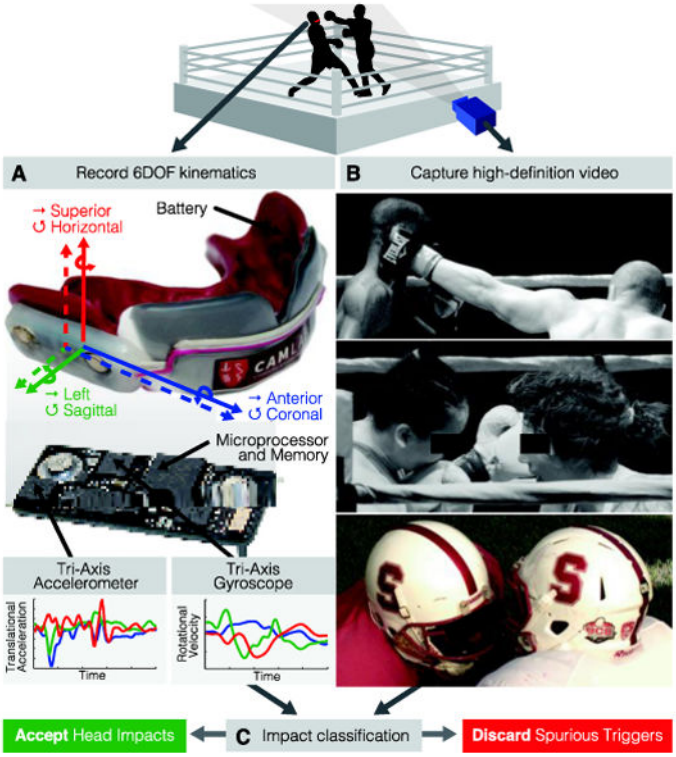

Fig 1. Mouthguard design and data acquisition

When an athlete experiences high head acceleration, we collect (**A**) six degree of freedom (6DOF) kinematic measurements using custom-fit mouthguards, and (**B**) time-stamped, high-definition video of all events to qualitatively study each impact and (**C**) confirm that device measurements correspond to true head impacts.

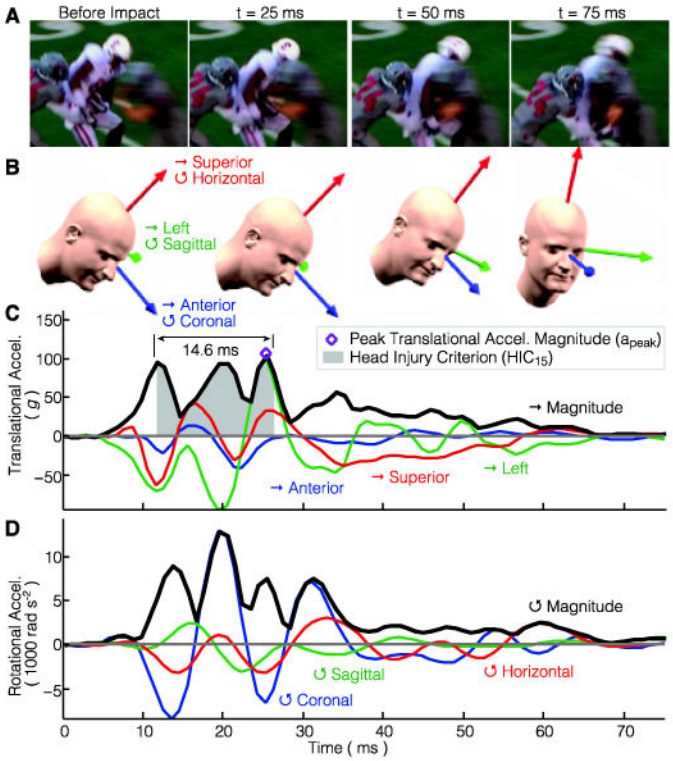

Fig 2. Measurement of human mild traumatic brain injury

A collegiate American football player lost consciousness after sustaining a head impact during a regular season game. (**A**) Broadcast footage at 40 frames s−1 are compared with an (**B**) animation of head position and orientation during the impact calculated by integrating (**C**) device measurements of translational acceleration and (**D**) rotational acceleration

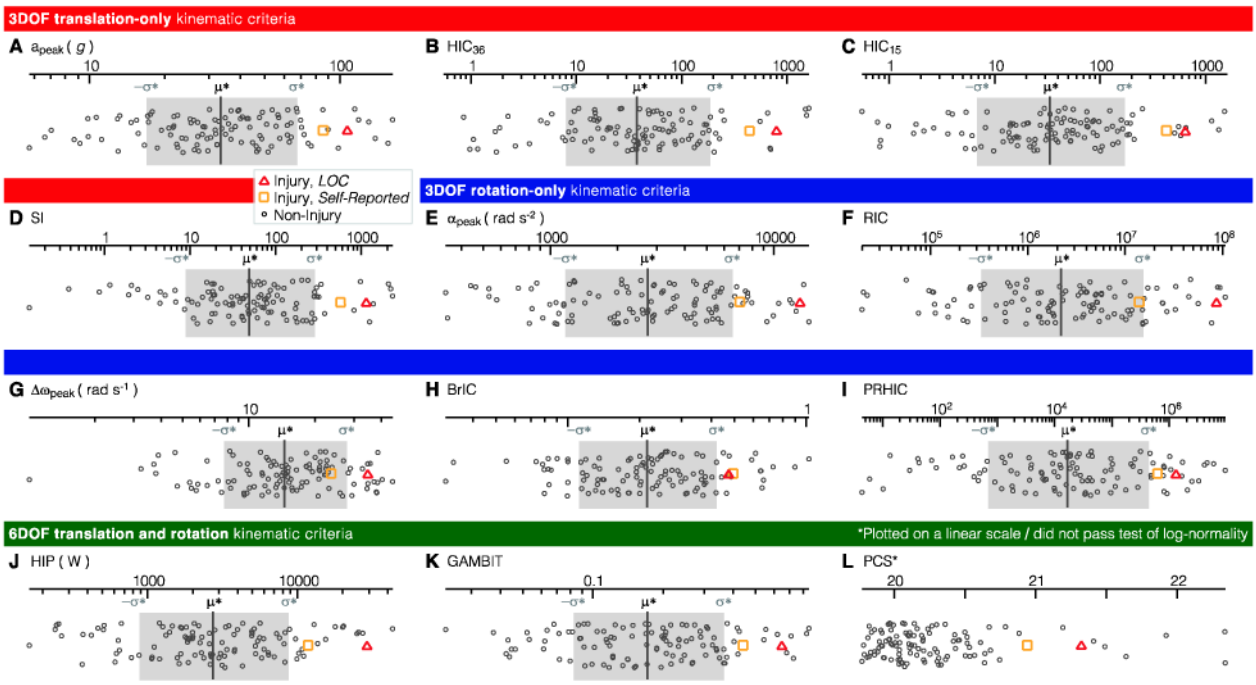

Fig 3. Kinematic injury criteria

Injury and non-injury values for each kinematic criteria are given for a subset of 110 impacts (2 injuries, 58 high acceleration, and 50 randomly-selected). All but PCS passed a Kolmogorov-Smirnov test of log-normality with statistical significance. The region that lies within one standard deviation, σ^*, of the log-normal median, μ^*, is indicated

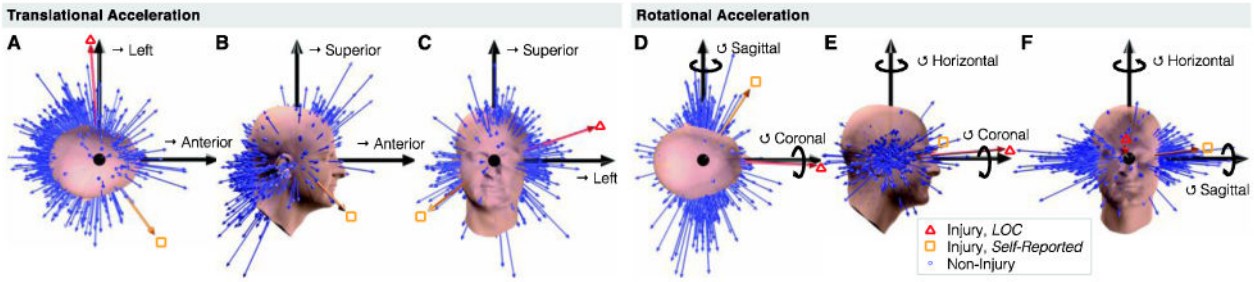

Fig 4. Direction of head acceleration

The direction of (**A-C**) peak translational acceleration, and (**D-F**) peak rotational acceleration distinguishes injury from non-injury. Most impacts resulted in posterior translation and sagittal plane rotation of the head.

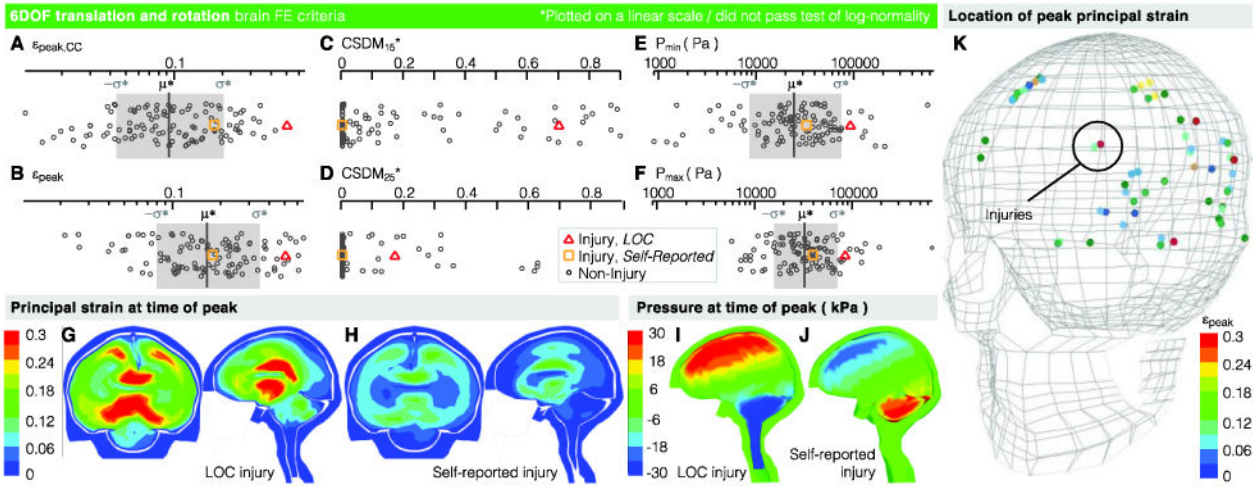

Fig 5. Brain deformation injury criteria

Injury and non-injury values for each (**A-F**) brain deformation criteria are given for the subset of 110 impacts. Multiplicative standard deviation, σ^*, and log-normal median, μ^*, are indicated (all criteria except CSDM passed a test of log-normality). Fringe plots of (**G-H**) principal strain and (**I-J**) pressure indicate regions of greatest brain deformation. (**K**) Peak principal strain in both injuries uniquely occurred in the corpus callosum.

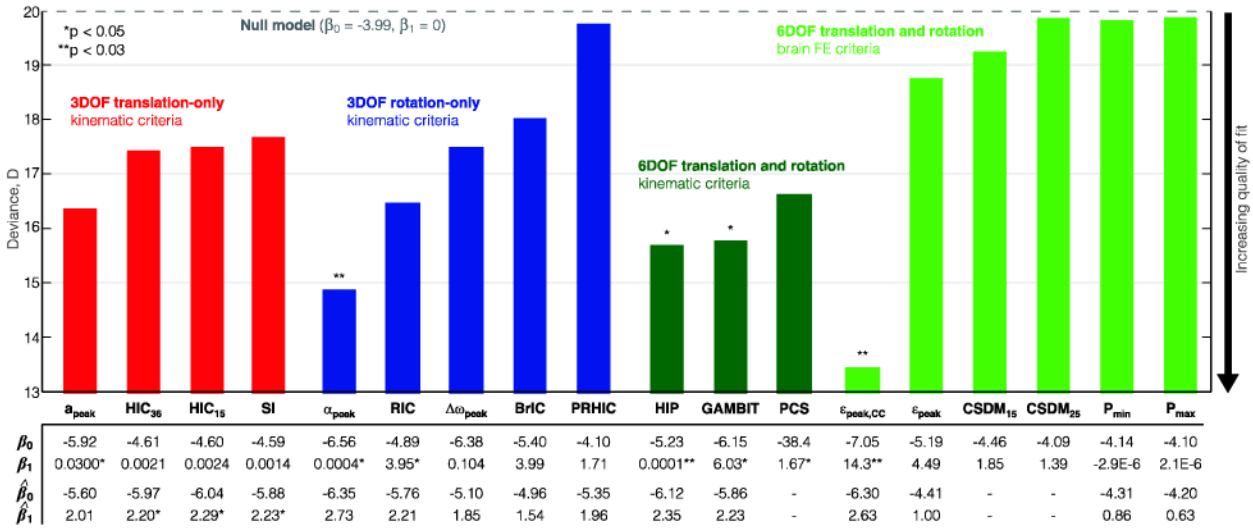

	a_{peak}	HIC_{36}	HIC_{15}	SI	α_{peak}	RIC	$\Delta\omega_{peak}$	BrIC	PRHIC	HIP	GAMBIT	PCS	$\varepsilon_{peak,CC}$	ε_{peak}	$CSDM_{15}$	$CSDM_{25}$	P_{min}	P_{max}
β_0	-5.92	-4.61	-4.60	-4.59	-6.56	-4.89	-6.38	-5.40	-4.10	-5.23	-6.15	-38.4	-7.05	-5.19	-4.46	-4.09	-4.14	-4.10
β_1	0.0300*	0.0021	0.0024	0.0014	0.0004*	3.95*	0.104	3.99	1.71	0.0001**	6.03*	1.67*	14.3**	4.49	1.85	1.39	-2.9E-6	2.1E-6
$\hat{\beta}_0$	-5.60	-5.97	-6.04	-5.88	-6.35	-5.76	-5.10	-4.96	-5.35	-6.12	-5.86	-	-6.30	-4.41	-	-	-4.31	-4.20
$\hat{\beta}_1$	2.01	2.20*	2.29*	2.23*	2.73	2.21	1.85	1.54	1.96	2.35	2.23	-	2.63	1.00	-	-	0.86	0.63

Fig 6. Injury prediction using logistic regression

Logistic model coefficients, β_0 and β_1 (β'_0 and β'_1 for standardized values), are given for 18 injury criteria. Decreasing deviance, D, suggests a criteria logistic regression more closely approximates a perfectly-predictive model. Criteria with deviance that significantly differed from the null model deviance are indicated by asterisks over their bar.

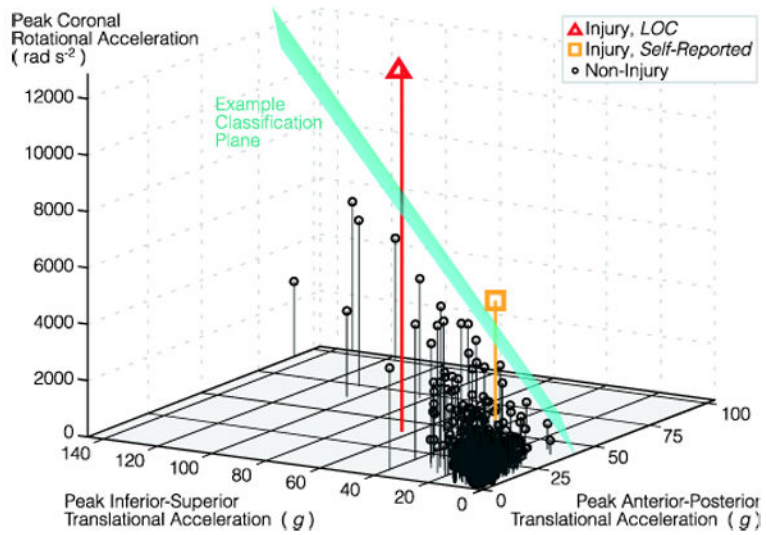

Fig 7. Example injury classification using machine learning

The LOC and self-reported injuries were separable from non-injury data using a three-dimensional hyperplane defined by two translational acceleration quantities and one rotational acceleration quantity. With few injury data points, this plane should not be interpreted to represent injury tolerance - additional injury data will certainly reveal injury classification bounds defined with more dimensions.

Table 1

Existing injury criteria

These 18 kinematic and brain finite element (FE) criteria have been proposed to predict mild traumatic brain injury (mTBI) using 3 or 6 degree of freedom (DOF) measurements. Half of these criteria use acceleration magnitude, which does not capture direction-dependent tolerance to injury.

Injury Criteria	Independently Measured DOF	Direction Dependence
3DOF translation-only *kinematic criteria*		
Peak Translational Acceleration Magnitude (a_{peak})[18,30,50,60,63,71]	3 (Translation)	No
Head Injury Criterion, Δt = 36 ms (HIC_{36})[21,45,51,63,78]	3 (Translation)	No
Head Injury Criterion, Δt = 15 ms (HIC_{15})[21,45,51,63,78]	3 (Translation)	No
Severity Index (SI)[7,8,23,51,63]	3 (Translation)	No
3DOF rotation-only *kinematic criteria*		
Peak Rotational Acceleration Magnitude (α_{peak})[37,48,61,63,72]	3 (Rotation)	No
Rotational Injury Criterion (RIC)[12,42]	3 (Rotation)	No
Peak Change in Rotational Velocity Magnitude ($\Delta\omega_{peak}$)[48,59,72]	3 (Rotation)	No
Brain Injury Criterion (BrIC)[75]	3 (Rotation)	Yes
Power Rotational Head Injury Criterion (PRHIC)[12,43]	3 (Rotation)	Yes
6DOF translation and rotation *kinematic criteria*		
Head Impact Power (HIP)[49,55]	6 (Trans & Rot)	Yes
Generalized Acceleration Model… (GAMBIT)[54]	6 (Trans & Rot)	No
Principal Component Score (PCS)[29]	6 (Trans & Rot)	No
6DOF translation and rotation *brain FE criteria*[*]		
Principal Strain, Corpus Callosum ($\varepsilon_{peak,CC}$)[16,47]	6 (Trans & Rot)	Yes
Principal Strain, Whole Brain (ε_{peak})[16,47]	6 (Trans & Rot)	Yes
Cumulative Strain Damage Measure ($CSDM_{15}$)[76]	6 (Trans & Rot)	Yes
Cumulative Strain Damage Measure ($CSDM_{25}$)[76]	6 (Trans & Rot)	Yes
Minimum Pressure (P_{min})[79]	6 (Trans & Rot)	Yes
Maximum Pressure (P_{max})[79]	6 (Trans & Rot)	Yes

[*] Criteria computed using finite element analysis with 6DOF measurement input

Table 2

Measurements of human head impacts

The present study includes the first direct six degree of freedom (6DOF) measurements of clinically-diagnosed mTBI. The incidence of a measured injury is rare, highlighting the present dataset and the difficulty of acquiring it. This list is not a comprehensive summary all studies reporting kinematic measurements, but rather, highlights first-of-its-kind measurements of human head impacts to the best of our knowledge; some of these devices, notably the Head Impact Telemetry (HIT) System [19], have been used to measure many more impacts (and injuries) in follow-up studies.

Study	Measurement Device	Sport Deployment	Independently Measured DOF	Number of Measured Injuries	Number of Measured Impacts	Video Confirmation of Impacts
Current study	Mouthguard-mounted sensors	Football, boxing, MMA	6DOF (Translation and rotation)	2	513	All
Pincemaille, et al. (1989)[64]	Headband-mounted sensors	Boxing	6DOF (Translation and rotation)	0	45	All
Pellman, et al. (2003)[63]	Dummy head sensors	Football	6DOF (Translation and rotation)	*25**	*31**	All
Rowson, et al. (2009)[70]	Helmet-mounted sensors	Football	6DOF (Translation and rotation)	0	1,712	None
Moon, et al. (1971)[50]	Headband-mounted sensors	Football	3DOF (Translation-only)	0	Unspecified	All
Reid, et al.(1974)[67]	Headband-mounted sensors	Football	3DOF (Translation-only)	1	650	Unspecified
Naunheim, et al. (2000)[53]	Helmet-mounted sensors	Football, hockey, soccer	3DOF (Translation-only)	0	344	All
Duma, et al. (2005)[19]	Helmet-mounted sensors	Football	3DOF (Translation-only)**	1	3,312	All

* Head impact kinematics deduced from laboratory reconstructions of game video,

** 2DOF rotation is inferred from the translation measurements

Table 3

Mouthguard accuracy and deployment

Over 3 years, subjects were instrumented with any of four mouthguard models with distinct form factor and sensor differences. A laboratory validation protocol 13 found strong correlation between mouthguard kinematics and dummy head reference sensors.

Mouthguard Design *Form Factor* (*Accel/Gyro*)	Translational Acceleration		Rotational Acceleration		Rotational Velocity		Number of Recorded Impact	Sport Usage
	m	r^2	*m*	r^2	*m*	r^2		
In-mouth (ADXL/L3G4)*	1.02	0.94	0.99	0.89	0.97	0.97	1**	Football
Cantilever tab (ADXL/L3G4)	1.01	0.96	0.90	0.89	1.00	0.98	117	Football
Cantilever tab (H3LI/L3G4)	0.95	0.95	0.98	0.89	0.99	0.97	292	Football
In-mouth (H3LI/ITG)	1.09	0.94	0.94	0.70	1.00	0.94	103***	All

* Accuracy validation performed on drop tester at nine heights and 17 impact locations

** Includes loss of consciousness (LOC) injury,

*** Includes self-reported injury